Journal of Sound and Vibration (1997) **205**(5), 671–688

MODAL COUPLING CONTROLLER DESIGN USING NORMAL FORM METHOD, PART II: CONTROL

A. KHAJEPOUR AND M. F. GOLNARAGHI

Department of Mechanical Engineering, University of Waterloo, Waterloo, Ontario N2L 3G1, Canada

AND

K. A. MORRIS

Department of Applied Mathematics, University of Waterloo, Waterloo, Ontario N2L 3G1, Canada

(*Received* 10 *January* 1996, *and in final form* 31 *March* 1997)

In part I [6] of this work the application of **M**odal **C**oupling **C**ontrol (MCC) to vibration control of oscillatory systems from a theoretical and computer simulation perspective was studied. A second order auxiliary system as the controller which was coupled to the plant through non-linear terms was developed. The general form of the coupling terms was derived, which showed that when the system is in resonance, a strong energy link between the plant and controller is established. A phenomenon called the *neck* resulting from the proposed method was also introduced.

In this part the neck phenomenon is studied in detail and shows that by using the proposed MCC, the neck exists for any non-linear second order system with oscillatory linear part. The stability of the closed loop system is also addressed and a relation for the selection of the controller gains for having a stable system is derived. Upon calculating the neck time analytically, an algorithm for control implementation is elaborated. Finally, the proposed controller is applied to an experimental cantilever flexible beam with piezo-ceramic actuators. The results show that the proposed controller is more effective than the conventional velocity feedback control specially when the control effort is unidirectional. This is particularly important for actuators which are not able to provide a bi-directional force such as cable-driven and shape memory alloy actuators.

1. INTRODUCTION

In this section the results obtained in reference [1] are reviewed. The authors then prove that there exists a neck in any non-linear second order system with oscillatory linear part. A relation that gives the time at which the neck occurs is derived. This relation enables one to apply the new controller strategy to a wide class of linear and non-linear systems.

In reference [1] a general second order differential equation was considered as the plant,

$$\dot{x}_p = A_p x_p + F_p(x_p) + U_p, \tag{1}$$

where $x_p = (x_{p1}, x_{p2})^{\mathrm{T}}$ is the span of the state variables, and

$$A_p = \begin{pmatrix} 0 & 1 \\ -w_p^2 & -2\zeta_p w_p \end{pmatrix}, \tag{2a}$$

0022–460X/97/350671 + 18 $25.00/0/sv971073

$$F_p(x_p) = \begin{pmatrix} f_1(x_p) \\ f_2(x_p) \end{pmatrix}, \qquad U_p = \begin{pmatrix} 0 \\ u_p \end{pmatrix}. \tag{2b}$$

The non-linear terms $f_1(x_p)$, $f_2(x_p)$ are continuous and differentiable and one assumes $f_1(0) = f_2(0) = 0$ and $Df_1(0) = Df_2(0) = 0$ to ensure that the origin is a fixed point. The plant input is U_p which is defined later.

Since the essence of the modal coupling controller is a strong interaction between two systems, another second order oscillatory system was defined as the controller:

$$\dot{x}_c = A_c x_c + U_c, \tag{3}$$

where $x_c = (x_{c1}, x_{c2})^{\mathrm{T}}$ and

$$A_c = \begin{pmatrix} 0 & 1 \\ -w_c^2 & -2\zeta_c w_c \end{pmatrix}, \qquad U_c = \begin{pmatrix} 0 \\ u_c \end{pmatrix}. \tag{4a, b}$$

The above two systems (1) and (3) are coupled through the input terms U_p and U_c. Assuming U_p and U_c are second order in x_p and x_c, one showed in reference [1] that the equations are strongly coupled when $w_c = w_p/(2\sqrt{1-\zeta_c^2})$ and $u_p(x)$ and $u_c(x)$ are chosen to be

$$u_p(x_c) = p_1 x_{c1}^2 + p_2 x_{c1} x_{c2} + p_3 x_{c2}^2, \tag{5a}$$

$$u_c(x_p, x_c) = q_1 x_{p1} x_{c1} + q_2 x_{p1} x_{c2} + q_3 x_{p2} x_{c1} + q_4 x_{p2} x_{c2}, \tag{5b}$$

where $p_1, \ldots, p_3$ and $q_1, \ldots, q_4$ are constant.

Defining a normal form transformation

$$x_p = y_p + h_2(y_c), \qquad x_c = y_c, \tag{6a, b}$$

where $h_2(y_c)$ is

$$h_2(y_c) = \begin{pmatrix} \delta_1 y_{c1}^2 + \delta_2 y_{c1} y_{c2} + \delta_3 y_{c2}^2 \\ \delta_1' y_{c1}^2 + \delta_2' y_{c1} y_{c2} + \delta_3' y_{c2}^2 \end{pmatrix}, \tag{7}$$

with coefficients given in reference [1], the equations (1) and (3) are transferred to

$$\dot{y}_p = A_p y_p + F_p(y_p) + \mathcal{O}(3), \qquad \dot{y}_c = A_c y_c + U_c(y) + \mathcal{O}(3) \tag{8a, b}$$

with initial conditions

$$x_p(0) = y_p(0) + h_2(y_c(0)), \qquad x_c(0) = y_c(0). \tag{9a, b}$$

Ignoring higher order terms, $\mathcal{O}(3)$, in equation (8a), the plant response in normal form space is zero if $y_p(0) = 0$. Therefore, knowing the plant initial conditions in $x_p(0)$, the authors suggested the initial conditions of the controller $y_c(0)$ be chosen so that $y_p(0) = 0$ or

$$x_p(0) = h_2(y_c(0)), \qquad x_c(0) = y_c(0). \tag{10a, b}$$

Using the feedback inputs (5) to couple two systems and choosing the controller initial conditions from equation (10), a strong energy link is established and the oscillatory energy is exchanged from the plant (1) to the controller (3) so that at a certain point the plant energy becomes minimum. This minimum point of the plant energy was called the *neck* and the time required to reach the neck *neck time*.

As an example, consider the following oscillatory system with non-linear damping and restoring force (note that in this example $\dot{x}_{p1} = x_{p2}$, $\dot{x}_{c1} = x_{c2}$, $f_1(x_p) = 0$ and $f_2(x_p) = -C\dot{x}_{p1}^3 - Kx_{p1}^3$:

$$\ddot{x}_{p1} + 2w_p\zeta_p\dot{x}_{p1} + w_p^2x_{p1} + C\dot{x}_{p1}^3 + Kx_{p1}^3 = u_p. \tag{11}$$

The plant input u_p is now used to couple equation (11) with another oscillatory system (the controller)

$$\ddot{x}_{c1} + 2w_c\zeta_c\dot{x}_{c1} + w_c^2x_{c1}^2 = u_c, \tag{12}$$

where $w_c = w_p/2\sqrt{1-\zeta_c^2}$ and u_c is the controller input. Using equation (5) and assuming $p_1 = 0$, $p_2 = 8$, $p_3 = -3$ and $q_1 = q_2 = 0$, $q_3 = -1$, $q_4 = 0{\cdot}4$, the plant and the controller inputs become (the stability of the closed loop system is investigated in section 4)

$$u_p = 8x_{c1}\dot{x}_{c1} - 3\dot{x}_{c1}^2, \qquad u_c = -\dot{x}_{p1}x_{c1} + 0{\cdot}4\dot{x}_{p1}\dot{x}_{c1}. \tag{13a, b}$$

To show the neck in the plant response, the system is simulated for the four cases shown in Table 1. For simplicity the initial conditions of the plant (11) are assumed to be $x_p = (0{\cdot}1, 0{\cdot}2)^{\mathrm{T}}$ for all cases.

Using equation (10) there are two solutions for $y_c(0)$ in each case study of Table 1. However, the solutions are only different in sign and therefore the controller response, $x_{c1}(t)$ and $x_{c2}(t)$, using either solution is the same except for a 180° phase difference. Since the plant input is second order in x_{c1} and x_{c2}, the plant response is not affected by the choice of either solutions.

Figure 1(a) is the plant response $x_{p1}(t)$ for case 1 that is a simple undamped linear oscillatory. As seen in the figure, the plant response decays to zero (the neck) and then rises to constant amplitude oscillations. The response of the system after changing the controller and plant damping and also adding non-linear terms to the system (case 2) is illustrated in Figure 1(b). As shown in the figure the occurrence of the neck is not affected by adding the non-linearities or by changing the damping ratios. The vertical lines in the figures show the approximated neck time which will be derived in the next section.

Finally, the plant natural frequency (w_p) is changed and the response of the system for a linear and non-linear case examined. Figures 2(a) and 2(b) demonstrate the response of the system for cases 3 and 4, respectively. In these cases the same behavior emerges in the plant response and the progression of the neck for a general non-linear system using the proposed method is evident.

In this paper, in order to take advantage of this phenomenon, the existence of the neck is first shown, in a class of non-linear systems defined by equations (1) and (3) and then a relation for the neck time in terms of the system parameter is dervied. The stability of the closed loop system is also proven and an algorithm for control implementation introduced. The method is then applied to an experimental piezo-actuated flexible beam. Previous research and literature relevant to this topic (references [2–11]) has been

TABLE 1

Parameters of equations (11) *and* (12)

Case	w_p	ζ_p	ζ_c	C	K	$x_{c1}(0)$	$\dot{x}_{c1}(0)$	$w_c = w_p/\sqrt{1-\zeta_c^2}$
1	20	0	0·15	0	0	0·145	2·699	10·11
2	20	0·01	0·1	0·03	200	0·113	1·955	10·05
3	10	0	0·15	0	0	0·098	1·383	5·06
4	10	0·01	0·1	0·02	40	0·077	1·012	5·03

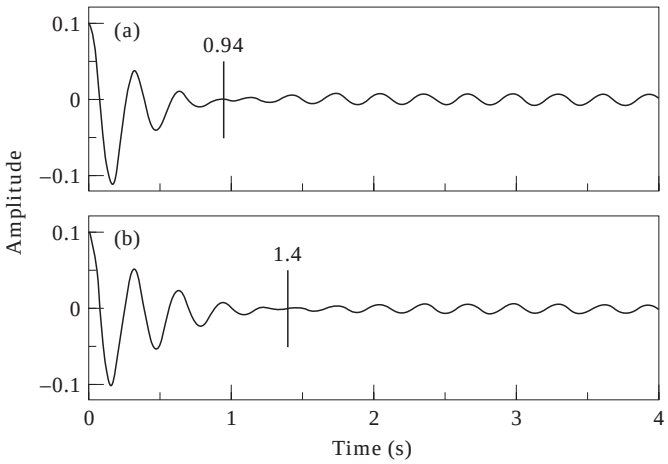

Figure 1. Plant response for (a) case 1 and (b) case 2 of Table 1.

summarized in part I. Other aspects of non-linear analysis and control are provided in references [13, 14].

2. ANALYSIS OF THE NECK

In order to use the neck as a mechanism to remove the oscillatory energy from the plant to the controller one should be able to address: (1) In what kind of systems does the neck exist? (2) How is the neck time related to the system parameters and the initial conditions?

The authors' tool in addressing the above questions and capturing the neck in the plant response is transformation (6) and the system normal form equation (8). Equation (8) is a non-linear system of differential equations and does not have a closed form solution. Also, assuming $y_p(0) = 0$, the solution of the truncated normal form (ignorning $\mathcal{O}(3)$ from equations (8)) is $y_p(t) = 0$ and $y_c(t) = e^{A_c t} y_c(0)$. Therefore, the plant response using $x_p = y_p + h_2(y_c)$ is a damped oscillatory response and does not predict a neck. The only way to capture the neck is to consider equation (8) with higher order terms. In the next

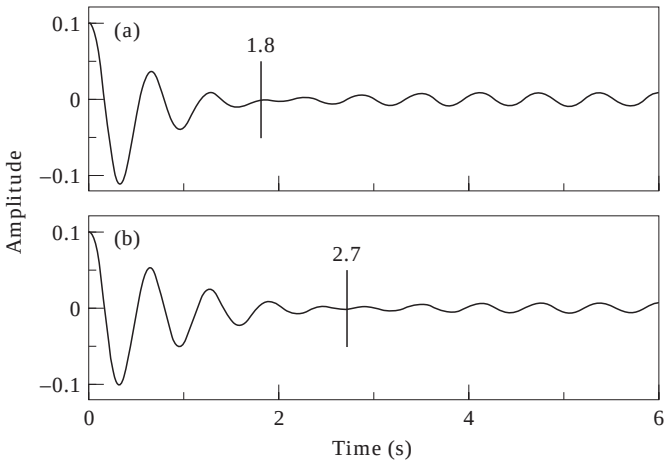

Figure 2. Plant response for (a) case 3 and (b) case 4 of Table 1.

section the higher order terms of equation (8) are derived and a perturbation method used to approximate the solution.

2.1. APPLYING PERTURBATION TO NORMAL FORM EQUATIONS

The non-linearity of the plant $F_p(x_p)$ is first expanded in a Taylor series

$$F_p(x_p) = F_p^2(x_p) + F_p^3(x_p) + \cdots, \tag{14}$$

where $F_p^i(x_p)$ is the ith order in the expansion. The quadratic term of $F_p(x_p)$ is written as

$$F_p^2(x_p) = \begin{pmatrix} x_p^{\mathrm{T}} R_1 x_p \\ x_p^{\mathrm{T}} R_2 x_p \end{pmatrix}, \tag{15}$$

where R_1 and R_2 are symmetric constant matrices

$$R_1 = \begin{pmatrix} r_1 & \frac{1}{2}r_2 \\ \frac{1}{2}r_2 & r_3 \end{pmatrix}, \qquad R_2 = \begin{pmatrix} r_1' & \frac{1}{2}r_2' \\ \frac{1}{2}r_2' & r_3' \end{pmatrix}. \tag{16}$$

Now the equations of the plant (1) and the controller (3) with inputs (5a) and (5b) and non-linear terms (14) are

$$\dot{x}_p = A_p x_p + U_p(x_c) + F_p^2(x_p) + F_p^3(x_p) + \mathcal{O}(4), \tag{17a}$$

$$\dot{x}_c = A_c x_c + U_c(x_c, x_p). \tag{17b}$$

Applying transformation (6) to equation (17) and observing that equation (6) eliminates $U_p(x_c)$, equation (17) is transformed into

$$\dot{y}_p = A_p y_p + F_p^2(y_p) + G_3(y_p, y_c) + \psi_4(y_c) + G_4(y_p, y_c) + \mathcal{O}(5), \tag{18a}$$

$$\dot{y}_c = A_c y_c + U_c(y_p + h_2(y_c), y_c), \tag{18b}$$

where $\psi_4(y_c)$ contains all fourth order terms of only y_c and $G_i(y_p, y_c)$ contains all other terms of order i. In the following analysis one only needs $\psi_4(y_c)$, that is

$$\psi_4(y_c) = \begin{pmatrix} h_2(y_c)^{\mathrm{T}} R_1 \\ h_2(y_c)^{\mathrm{T}} R_2 \end{pmatrix} h_2(y_c) - 2 \begin{pmatrix} \frac{1}{2}\delta_2 & \delta_3 \\ \frac{1}{2}\delta_2' & \delta_3' \end{pmatrix} y_c h_2(y_c)^{\mathrm{T}} Q y_c. \tag{19}$$

Equation (18) is non-linear and more complicated than equation (17). However, in the proposed control scheme the initial conditions of the plant in equation (18a) are zero. This assists one to find an approximate solution for equation (18) using a perturbation method.

One first scales equation (18) and transformation (6). Considering ϵ as a positive but small parameter, equation (18) becomes

$$\dot{y}_p = A_p y_p + \epsilon(F_p^2(y_p) + G_3(y_p, y_c) + \psi_4(y_c) + G_4(y_p, y_c) + \mathcal{O}(5)), \tag{20a}$$

$$\dot{y}_c = A_c y_c + \epsilon U_c(y_p + h_2(y_c), y_c), \tag{20b}$$

and equation (6) is written

$$x_p = y_p + \epsilon h_2(y_c). \tag{21}$$

Using the fact that the solution of equation (20) is analytic with respect to parameter ϵ (see e.g., Nayfeh and Mook [14]), y_p and y_c can be written as a power series expansion in ϵ:

$$y_p = y_p^{(0)}(t) + \epsilon y_p^{(1)}(t) + \cdots + \epsilon^n y_p^{(n)}(t) + \cdots, \tag{22a}$$

$$y_c = y_c^{(0)}(t) + \epsilon y_c^{(1)}(t) + \cdots + \epsilon^n y_c^{(n)}(t) + \cdots. \tag{22b}$$

The coefficients of the powers of the parameter ϵ are functions of the independent variable t. The functions $y_p^{(n)}(t)$ and $y_c^{(n)}(t)$ are found by substituting equation (22) into equation (20) and equating the coefficients of like powers of ϵ. This leads to an infinite set of linear inhomogeneous differential equations that may be solved recursively.

Substituting equation (22) into equation (20) and collecting terms of the same power of ϵ, one obtains

ϵ^0:

$$\dot{y}_p^{(0)} = A_p y_p^{(0)}, \qquad \dot{y}_c^{(0)} = A_c y_c^{(0)}. \tag{23a, b}$$

ϵ^1:

$$\dot{y}_p^{(1)} = A_p y_p^{(1)} + F_p^2(y_p^{(0)}) + G_3(y_p^{(0)}, y_c^{(0)}) + \psi_4(y_c^{(0)}) + G_4(y_p^{(0)}, y_c^{(0)}) + \mathcal{O}(5), \tag{24a}$$

$$\dot{y}_c^{(1)} = A_c y_c^{(1)} + U_c(y_p^{(0)} + h_2(y_c^{(0)}), y_c^{(0)}). \tag{24b}$$

Using the solutions of equations (23) and (24) in equation (21) one obtains

$$x_p = y_p^{(0)} + \epsilon y_p^{(1)} + \cdots + \epsilon h_2(y_c^{(0)} + \epsilon y_c^{(1)} + \cdots) = y_p^{(0)} + \epsilon(y_p^{(1)} + h_2(y_c^{(0)})) + \cdots. \tag{25}$$

Since in the proposed control scheme $y_c(0)$ has been chosen so that $y_p(0) = 0$, the initial conditions of equation (20) under the substitution (22) translate into the following initial conditions on the coefficients $y_p^{(n)}(t)$ and $y_c^{(n)}(t)$:

$$y_p^{(n)}(0) = 0, \quad n \geqslant 0; \qquad y_c^{(n)}(0) = \begin{cases} y_c(0), & n = 0 \\ 0, & n \geqslant 1 \end{cases}. \tag{26a, b}$$

The solution of equation (23) with associated initial conditions from equation (26) is

$$y_p^{(0)}(t) \equiv 0, \qquad y_c^{(0)}(t) = \mathrm{e}^{A_c t} y_c(0). \tag{27a, b}$$

One substitutes equation (27) into equation (24) to obtain a non-homogeneous differential equation for $y_p^{(1)}$. Ignoring $\mathcal{O}(5)$ and noticing that $y_p^{(0)}(t) \equiv 0$, one obtains

$$\dot{y}_p^{(1)} = A_p y_p^{(1)} + \psi_4(y_c^{(0)}(t)), \qquad y_p^{(1)}(0) = 0. \tag{28}$$

The solution of linear non-homogeneous equation (28) with zero initial condition is

$$y_p^{(1)}(t) = \int_0^t \mathrm{e}^{A_p(t-\tau)} \psi_4(y_c^{(0)})\, \mathrm{d}\tau. \tag{29}$$

The plant response can now be approximated (setting $\epsilon = 1$) by

$$x_p = y_p^{(1)}(t) + h_2(y_c^{(0)}). \tag{30}$$

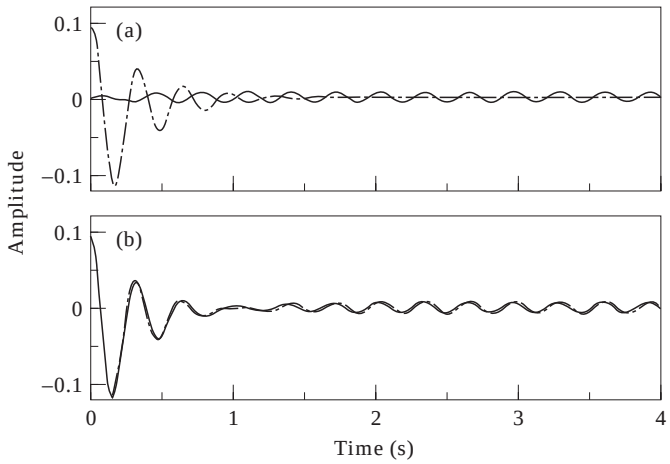

Figure 3. (a) Approximate plant response: $y_{p1}^{(1)}$ (——), $h_{21}(y_c^{(0)})$ (— - —). (b) Exact solution (——), approximate solution (— - —).

The approximated plant response in equation (30) consists of two terms. The first term, $y_p^{(1)}(t)$ in equation (29), evolves from zero to a periodic response with the plant natural frequency w_p. The second term $h_2(y_c^{(0)})$ starts at the plant initial conditions ($x_p(0) = h_2(0)$) and decays to zero since $h_2(\cdot)$ is a function of y_c.

As an example, consider case 1 in Table 1. In Figure 3(a), the solid line shows $y_{p1}^{(1)}(t)$, while the dashed line shows $h_{21}(y_c^{(0)})$ (note that $h_2(y_c) = (h_{21}(y_c), h_{22}(y_c))^{\mathrm{T}}$). Adding $y_{p1}^{(1)}(t)$ and $h_{21}(y_c^{(0)})$ results in the approximated plant response $x_{p1}(t)$ which is shown in Figure 3(b) with a dashed line. To compare the exact solution with the approximated solution, the plant response is plotted in Figure 3(b) with a solid line. The differences between the solutions are negligible and indicate the success of the analysis in explaining the neck phenomenon.

As seen in Figure 3(a) the phase difference $h_{21}(y_c^{(0)})$ and $y_{p1}^{(1)}(t)$ is almost 180°. Therefore, the addition of the responses of $h_{21}(y_c^{(0)})$ and $y_{p1}^{(1)}(t)$ causes a neck in the plant response. Figure 4 shows the envelopes of $h_{21}(y_c^{(0)})$ (curve 1) and $y_{p1}^{(1)}(t)$ (curve 2) along with the plant response (curve 3). It is clear from Figure 4 that the neck time is the time that the envelopes of $y_{p1}^{(1)}(t)$ and $h_{21}(y_c^{(0)})$ intersect. This fact is used to derive the neck time in the next section.

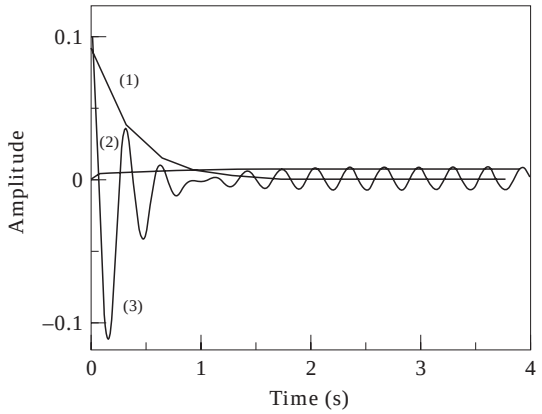

Figure 4. (1) Envelope of $h_{21}(y_c^{(0)})$, (2) envelope of $y_{p1}^{(1)}(t)$, (3) plant response.

3. CALCULATION OF THE NECK TIME

In this section the envelopes of $y_{p1}^{(1)}(t)$ and $h_{21}(y_c^{(0)})$ are approximated in order to find the neck time. We write the solution of $y_c^{(0)}(t)$, equation (27b), as

$$y_c^{(0)}(t) = Y_0 \, \mathrm{e}^{-\zeta_c w_c t} \begin{pmatrix} \sin(\beta_c w_c t + \phi_c) \\ w_c(-\zeta_c \sin(\beta_c w_c t + \phi_c) + \beta_c \cos(\beta_c w_c t + \phi_c)) \end{pmatrix}, \tag{31}$$

where (note that $y_c = (y_{c1}, y_{c2})^{\mathrm{T}}$ and $y_c^{(0)}(0) = y_c(0)$)

$$\phi_c = \tan^{-1}(\beta_c w_c y_{c1}(0)/[y_{c2}(0) + \zeta_c w_c y_{c1}(0)]), \qquad Y_0 = |y_{c1}(0)/\sin(\phi_c)|. \tag{32a, b}$$

Substitution of equation (31) into $h_{21}(\cdot)$, equation (7), and simplification, result in a damped oscillatory response for $h_{21}(y_c^{(0)})$ with frequency $2\beta_c w_c = w_p$ and damping factor $\mathrm{e}^{-2\zeta_c w_c t}$. Noticing that $w_p \approx 2w_c$ and $\mathrm{e}^{-2\zeta_c w_c t} \approx \mathrm{e}^{-\zeta_c w_p t}$, one can approximate $h_2(y_c^{(0)})$ with a one-degree-of-freedom system with frequency w_p and damping ratio ζ_c. Since $h_2(y_c^{(0)}(0)) = x_p(0)$ the envelope of $h_{21}(y_c^{(0)})$, env$(\cdot)$, is approximated as

$$\mathrm{env}\,(h_{21}(y_c^{(0)})) = X_0 \, \mathrm{e}^{-\zeta_c w_p t}, \tag{33}$$

where

$$\phi_p = \tan^{-1}(\beta_c w_p x_{p1}(0)/[x_{p2}(0) + \zeta_c w_p x_{p1}(0)]), \qquad X_0 = |x_{p1}(0)/\sin(\phi_p)|. \tag{34a, b}$$

To find the envelope of $y_p^{(1)}(t)$ one solves equation (28). Substituting $y_c^{(0)}$ from equation (31) into $\psi_4(y_c)$, equation (19), gives the forcing input of equation (28).

Since ζ_p in general is very small and negligible compared to ζ_c, equation (28) is solved assuming $\zeta_p = 0$. However, the effect of ζ_p is incorporated in the envelope of equation (28) later. Expansion of $\psi_4(y_c^{(0)})$ shows that it is composed of sin $(\cdot)$ and cos $(\cdot)$ with frequencies w_p and $2w_p$ and a constant term all of which are exponentially damped with factor $\mathrm{e}^{-4\zeta_c w_c t}$.

Equation (28) is solved for each individual term of $\psi_4(y_c^{(0)})$ and the final solution is found by superposition. Due to the volume of computation, a symbolic computation software, Maple, was used to derive and simplify the results†. The solution of (28) has the form (note that $y_p^{(1)}(t) = (y_{p1}^{(1)}, y_{p2}^{(1)})^{\mathrm{T}}$)

$$\begin{aligned} y_{p1}^{(1)}(t) = \mathrm{e}^{-4\zeta_c w_c t} Y_0^4 (k_1 \cos(w_p t + 2\phi_c) + k_2 \sin(w_p t + 2\phi_c) + k_3 \cos(2w_p t + 4\phi_c) \\ + k_4 \sin(2w_p t + 4\phi_c) + k_5) + \chi, \end{aligned} \tag{35}$$

where

$$\chi = (Y_0^4/d)(a \cos(w_p t) + b \sin(w_p t)) \tag{36}$$

and $k_1, \ldots, k_5$ and a, b, d are constants. The steady state response of equation (35), χ, is periodic and undamped and its envelope is $(Y_0^4/d)\sqrt{a^2 + b^2}$. The other terms of equation (35) decay to zero exponentially with damping factor $\mathrm{e}^{-4\zeta_c w_c t}$. Noticing that $y_{p1}^{(1)}(0) = 0$, the envelope of these terms is $-(Y_0^4/d)\sqrt{a^2 + b^2}\,\mathrm{e}^{-4\zeta_c w_c t}$. Addition of this envelope to the envelope of χ results in the envelope of $y_{p1}^{(1)}(t)$ that is

$$\mathrm{env}\,(y_{p1}^{(1)}(t)) = (Y_0^4/d)\sqrt{a^2 + b^2}(1 - \mathrm{e}^{-4\zeta_c w_c t}). \tag{37}$$

Equation (37) is the envelope of $y_{p1}^{(1)}(t)$ when $\zeta_p = 0$. However, by including the effect of the plant damping, noticing that when $\zeta_p \ll 1$, χ is written

$$\chi = (Y_0^4/d)(a \cos(w_p t) + b \sin(w_p t)) \, \mathrm{e}^{-\zeta_p w_p t}, \tag{38}$$

† All calculations in Maple are available upon request.

its envelope becomes $(Y_0/d)\sqrt{a^2+b^2}\,\mathrm{e}^{-\zeta_p w_p t}$. Therefore, the adjusted envelope of $y_{p1}^{(1)}(t)$ for $\zeta_p \neq 0$ is

$$\mathrm{env}\,(y_{p1}^{(1)}(t)) = (Y_0^4/d)\sqrt{a^2+b^2}(\mathrm{e}^{-\zeta_p w_p t} - \mathrm{e}^{-4\zeta_c w_c t}). \tag{39}$$

The expressions for a and b are complicated. However, a and b are polynomials of ζ_c and ignoring all terms but the linear terms, gives a very good approximation for the envelope of $y_{p1}^{(1)}(t)$. This approximated envelope takes the form

$$\mathrm{env}\,(y_{p1}^{(1)}) = (Y_0^4/d)\sqrt{(a_0+a_1\zeta_c)^2+(b_0+b_1\zeta_c)^2}(\mathrm{e}^{-\zeta_p w_p t} - \mathrm{e}^{-4\zeta_c w_c t}). \tag{40}$$

Including the stability analysis results which are derived in the next section, a_0, a_1, b_0, b_1 and d are given in Appendix A. The expressions are specially simple when there are no second order non-linearities ($r_i = r_i' = 0$).

One can now use equations (33) and (40) to calculate the neck time. In Figure 4 one showed that the neck occurs when the envelopes of $h_{21}(y_c)$ and $y_{p1}(t)$ intersect. Using equations (33) and (40) to find the intersection of the envelopes of $h_{21}(y_c^{(0)})$ and $y_{p1}^{(1)}(t)$ yields

$$X_0 d/Y_0^4\sqrt{(a_0+a_1\zeta_c)^2+(b_0+b_1\zeta_c)^2} = \mathrm{e}^{-w_p(\zeta_p-\zeta_c)t_N} - \mathrm{e}^{-w_p(\zeta_c/\beta_c)(2-\beta_c)t_N}. \tag{41}$$

The value of t_N satisfying equation (41) is the neck time.

The case studies in Table 1 are now used to show the validity of the above analysis. In cases 1 and 3 of Table 1, $\zeta_p = 0$, and as seen in Figures 1(a) and 2(a) the plant responses have permanent oscillations. The amplitude of this permanent oscillation is approximated by equation (40) as $t \to \infty$. Column 2 in Table 2 displays the exact amplitude of the permanent oscillation while column 3 is the amplitude calculated using equation (40). The error between the exact and the approximated amplitudes is small. The neck time in column 4 of Table 2 is found using equation (41). The neck time is marked with a vertical line in the simulation results shown in Figures 1 and 2. The closeness of the approximated neck time to the exact time indicates the accuracy of the method.

So far, the existence of the neck in a class of non-linear systems defined in equations (1) and (3) has been shown. A relation to obtain the neck time has also been derived. In the subsequent section the stability of the closed loop system is studied and then the neck time is used to introduce an algorithm to implement the controller.

4. STABILITY ANALYSIS

In any controller design one of the main issues to be addressed is stability. If ζ_p and ζ_c are non-zero, Lyapunov's first method applied to equations (1) and (3) reveals that the origin of the closed loop system is stable. However, the controller scheme proposed in section 3.1 is for systems with $\zeta_p = 0$ or $\zeta_p \ll 0$. Using Lyapunov's second method we analyze the stability of equations (1) and (3) at the origin when $\zeta_p = 0$.

TABLE 2

Neck time and permanent amplitude

Case	Exact permanent amplitude	Approximated permanent amplitude using (40)	Neck time
1	0·007	0·006	0·94
2	0	0	1·44
3	0·008	0·007	1·77
4	0	0	2·73

The basic concept of Lyapunov's direct method is to find a continuously differentiable locally positive definite function V such that its derivative along the trajectories is locally negative semi-definite. In such cases the equilibrium point is stable.

It should be noted that the Lyapunov's second method provides only a sufficient condition for stability and no definite conclusion can be drawn if the derivative of V fails to be locally negative definite. Lyapunov's second method is not constructive, and there is no general rule to find a Lyapunov's function for any non-linear system.

Due to these difficulties our study is limited to the case when the plant non-linearity is of the form

$$F_p(x_p) = \begin{pmatrix} -g_1(x_p) \\ -g_2(x_{p1}) - g_3(x_p) \end{pmatrix}, \tag{42}$$

where $DF_p(0) = 0$ and, $g_1(x_p)$, $g_2(x_{p1})$ and $g_3(x_p)$ satisfy (1) g_1, g_2 and g_3 are continuous, (2) $g_1(0) = g_2(0) = g_3(0) = 0$, and (3) $x_{p1}g_1(x_p) > 0$, $x_{p1}g_2(x_{p1}) > 0$ and $x_{p2}g_3(x_p) > 0$ whenever x_{p1} and x_{p2} are non-zero. This form of non-linearity includes non-linear springs and non-linear viscous forces which are important in physical systems.

The closed loop equations (1) and (3) with non-linear terms (42) and inputs U_p and U_c given by equations (5a) and (5b) are now considered. One defines the Lyapunov's function candidate

$$V(x) = \tfrac{1}{2}x^{\mathrm{T}}Lx + a_1 \int_0^{x_{p1}} g_2(\xi)\,\mathrm{d}\xi, \tag{43}$$

where L is diagonal:

$$L = \mathrm{Diag}\,(a_1 w_p^2 \quad a_1 \quad a_2 w_c^2 \quad a_2) \tag{44}$$

and $a_1, a_2 > 0$. Conditions (1)–(3) ensure that V is a continuously differentiable positive definite function, so that V is a suitable Lyapunov's function candidate.

Calculating $\dot{V}(x)$, one obtains

$$\begin{aligned} \dot{V}(x) = {} & -a_1 w_p^2 x_{p1} g_1(x_p) - a_1 x_{p2} g_3(x_p) - 2a_2 w_c \zeta_c x_{c2}^2 - a_1 g_1(x_p) g_2(x_{p1}) \\ & + a_1 x_{p2} U_p + a_2 x_{c2} U_c. \end{aligned} \tag{45}$$

The first four terms in equation (45) are negative. The last two terms are cubic in x and therefore the origin is a saddle point. The only way to satisfy $\dot{V}(x) \leqslant 0$ is to set

$$a_1 x_{p2} U_p + a_2 x_{c2} U_c = 0. \tag{46}$$

Substituting U_p and U_c from equations (5a) and (5b) into equation (46) implies that

$$\begin{aligned} & a_1 p_1 x_{p2} x_{c1}^2 + a_2 q_1 x_{p1} x_{c1} x_{c2} + a_2 q_2 x_{p1} x_{c2}^2 \\ & \quad + (a_1 p_2 + a_2 q_3) x_{p2} x_{c1} x_{c2} + (a_1 p_3 + a_2 q_4) x_{p2} x_{c2}^2 = 0. \end{aligned} \tag{47}$$

Since a_1 and a_2 are non-zero,

$$p_1 = q_1 = q_2 = 0, \qquad a_1 p_2 + a_2 q_3 = 0, \qquad a_1 p_3 + a_2 q_4 = 0. \tag{48a–c}$$

The last two equations (48b) and (48c) can be simplified by recalling that a_1 and a_2 are positive. Since equations (48b) and (48c) have a solution for positive a_1 and a_2 if $p_2 q_3 \leqslant 0$ and $p_3 q_4 \leqslant 0$, the closed loop system is stable if equation (48a) holds and $p_2 q_3 \leqslant 0$ and $p_3 q_4 \leqslant 0$. Including equation (48a) in the plant and the controller inputs (5) simplifies the expression of a_0, a_1, b_0, b_1 and d which are given in Appendix A.

It should be noted that equation (48) is based on the Lyapunov's function defined in equation (43). The stability analysis was intended to give a simple (but possibly not general) relation for choosing the input gains so that the closed loop system becomes stable.

To this end the stability of the fixed point of equations (1) and (3) has been studied and a relation with which the input gains (p_i, q_i) are chosen for a stable system derived. In the next section using the proposed control strategy one shows that this method can be used to suppress the plant vibrations.

5. CONTROLLER IMPLEMENTATION

To implement the controller and take advantage of the neck phenomenon, the **U**pdating **I**nput **A**lgortihm (UIA) is introduced. In this algorithm the controller initial conditions are set (using equation (10)) so that the neck in the plant response is developed. Then the plant input $U_p(x_c)$ is applied until the plant response reaches the neck. At this time the controller is updated to cause a new neck in the system. This process continues until an acceptable amplitude in the plant response is obtained.

The steps of UIA are as follows:

(1) The plant states x_p are measured (sensors signals).
(2) The plant maximum amplitude, using equation (34), is calculated and compared with a small and acceptable reference value. This acceptable amplitude clearly depends on the application of the controller. If the amplitude is small enough then go to step (1), otherwise continue.
(3) The controller states x_c are found using equation (10).
(4) The neck time (t_N) is found using equation (41).
(5) The input $U_p(x_c)$ is applied to the plant for a period of t_N.
(6) Go to step (1).

To examine the above algorithm one applies it to the first two cases of Table 1. Figure 5(a) illustrates the response of the controlled plant x_{p1} with the proposed controller. The controller damping in this case is 0·15 and the plant is an undamped linear second order system. The plant input u_p is given in Figure 5(b) and indicates that the input is not

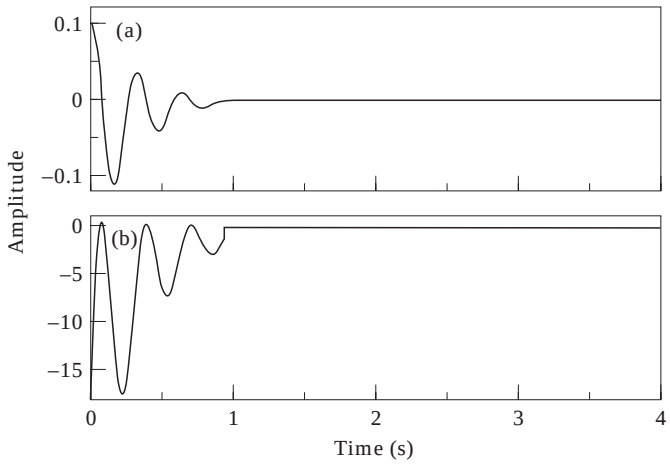

Figure 5. Case 1 of Table 1: (a) plant response, (b) plant input.

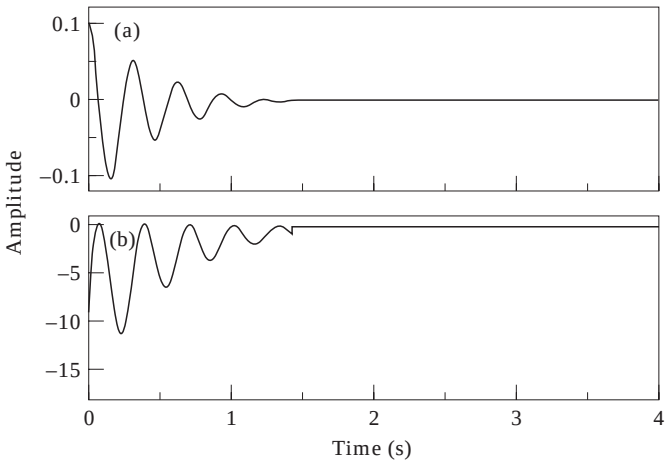

Figure 6. Case 2 of Table 1: (a) plant response, (b) plant input.

updated after the first neck. This is due to the fact that the plant amplitude at the neck is small enough for terminating the above algorithm in step (2).

The input in the proposed MCC can be chosen so that it becomes uni-directional. Since cable-driven actuators and shape memory alloys can apply force only in one direction, having a uni-directional input is a significant advantage of the proposed technique over the existing methods.

One showed that the neck phenomenon exists in any non-linear systems with oscillatory (damped or undamped) linear part. This indicates that the controller can be applied to a wide class of non-linear systems. Figure 6(a) is the response of the plant for the non-linear case illustrated in case 2 of Table 1. The plant input u_p for the proposed controller is shown in Figure 6(b).

In the next section an experimental piezo-actuated flexible beam is used to authenticate the theoretical results developed in reference [1] and this work. For simplicity, the flexible beam is modeled as a one-degree-of-freedom system and its natural frequency and damping ratio are obtained using experimental data. The controller is the proposed MCC with updating input algorithm UIA.

6. EXPERIMENTAL STUDY

The experimental system comprises a piezo-actuated cantilever beam, controlled digitally using a personal computer. The controller is implemented on software using "C" code. The beam is made of sheet aluminum with geometrical and physical properties as in Table 3. The actuator is composed of eight pieces of piezo-ceramic (Sensor HiTech Ltd., BM532) rigidly bonded to both sides of the aluminum sheet at the clamped end as shown

TABLE 3

Beam properties

Length (mm)	Width (mm)	Thickness (mm)	Density (kg/m^3)	Young's modulus (N/m^2)
457	25·5	0·8	2710	$7{\cdot}0 \times 10^{10}$

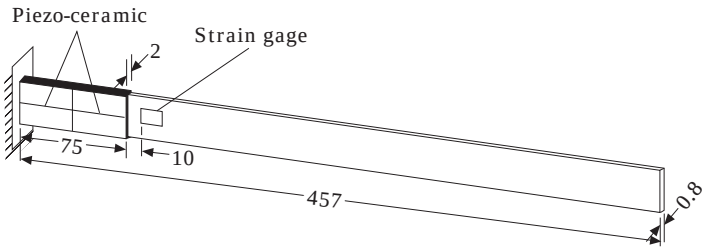

Figure 7. The experimental cantilever beam.

in Figure 7. The total length of the piezo-ceramic layers on each side is 75 mm with a thickness of 0·6 mm.

The beam deflection is measured using a strain gauge (Measurement Group Gauge, type EA-B-125TQ-350) bonded near the piezo-ceramic layers as seen in Figure 7. The beam is fixed to a massive test-bed in order to isolate the beam from external excitations.

The strain gauge signal is amplified using an in-house amplifier. In addition, for noise reduction the signal is filtered by a low pass filter with a cut-off frequency of 50 Hz. The signal is then converted to a digital signal using an A/D converter and sent to a personal computer.

The beam velocity is approximated numerically by a second order finite difference derivative using the beam deflection signal from the strain gauge. The beam state variables, position and velocity, are used to generate the feedback input using the proposed controller. After converting the plant input to an analog signal, the input is amplified and sent to the piezo-ceramic actuators.

The beam is considered as a one-degree-of-freedom system which is a simplified version of equation (1). That is,

$$\ddot{x}_{p1} + 2w_p\zeta_p\dot{x}_{p1} + w_p^2 x_{p1} = u_p, \tag{49}$$

where w_p and ζ_p are the natural frequency and damping ratio of the beam's first mode and u_p is the feedback input.

The natural frequency and damping ratio of the beam are determined using a time response of a free vibration of the beam. Figure 8(a) shows the beam response for a typical free vibration. Using Fourier transforms the frequency of the beam is obtained to be 27·0 rad/s or 4·30 Hz. To attempt to ascertain the beam damping ratio, one uses the logarithmic decrement technique for the beam time response shown in Figure 8(a). Since the damping is small one assumes $\sqrt{1-\zeta_p^2} \approx 1$. Implementing the logarithmic decrement method to the beam response every four cycles results in Figure 8(b). As the figure shows, the damping ratio declines as the beam amplitude decreases. This is explained by recognizing that due to light damping of the beam, air resistance is a major damping factor for vibration suppression. In addition, air resistance is a non-linear function of velocity and increases rapidly with velocity. Therefore, for large amplitudes where the beam travels faster the equivalent damping ratio obtained from the logarithmic decrement method is much higher than that for small oscillations. Since the damping ratio of the beam in general is very small an average value of $\zeta_p = 0{\cdot}004$ is assumed for the experimental work.

Identifying the beam equation, one now implements the proposed controller. As mentioned earlier the controller has the structure

$$\ddot{x}_{c1} + 2w_c\zeta_c\dot{x}_{c1} + w_c^2 x_{c1} = u_c, \tag{50}$$

where w_c and ζ_c are the controller natural frequency and damping ratio, respectively, and u_c is the feedback input. The controller frequency is set to resonance i.e. $w_c = w_p/2\sqrt{1-\zeta_c^2}$, while ζ_c mainly depends on the maximum capacity of the actuator. Larger ζ_c is an indication of faster vibration suppression or larger actuator effort. It should be noted that the bending moment applied by the actuator to the beam is directly proportional to the input voltage applied to the piezo-ceramics. The maximum voltage in our experiment is limited to 180 V which limits the maximum damping ζ_c.

The feedback inputs u_p and u_c are

$$u_p = p_2\dot{x}_{c1}x_{c1} + p_3\dot{x}_{c1}^2, \qquad u_c = q_3\dot{x}_{p1}x_{c1} + q_4\dot{x}_{p1}\dot{x}_{c1}, \tag{51a, b}$$

with $p_2q_3 \leqslant 0$ and $p_3q_4 \leqslant 0$ for closed loop stability. For this experiment one sets $p_2 = 0$, $p_3 = -1$, $q_3 = 0$, $q_4 = 2$ and assumes the beam tip oscillations do not exceed ± 40 mm. Applying the controller to the beam and measuring the input voltage to the piezo-ceramics shows that ζ_c cannot be more than 3·5%. Therefore, to use the full strength of the actuators one sets $\zeta_c = 0{\cdot}035$.

Selecting the controller initial conditions from equation (10) one demonstrated that a neck emerges in the plant response. In the following the authors first show the existence of the neck in the flexible beam response and then apply the proposed MCC to suppress the beam oscillations.

Figure 9(a) shows the beam response when the controller initial conditions are obtained using equation (10). As expected from the theory the beam oscillatory energy is transferred to the controller and then a portion of the energy is transferred back to the beam. Figure 9(b) presents the input voltage to the piezo-ceramics which is uni-directional (between -180 and 0 V).

To implement the proposed control strategy one uses the UIA. The beam response using UIA is shown in Figure 10(a) for an arbitrary initial condition. The piezo-actuator input in Figure 10(b) indicates that the input is updated when the beam response reaches its first neck, at around 2·1 s.

One of the present main achievements is the extension of MCC so that it can be used on-line. This was achieved by finding the controller initial conditions and the neck time analytically rather than using trial and error. To explore this capability of the proposed controller the controller was applied to the beam while it is repeatedly disturbed as shown

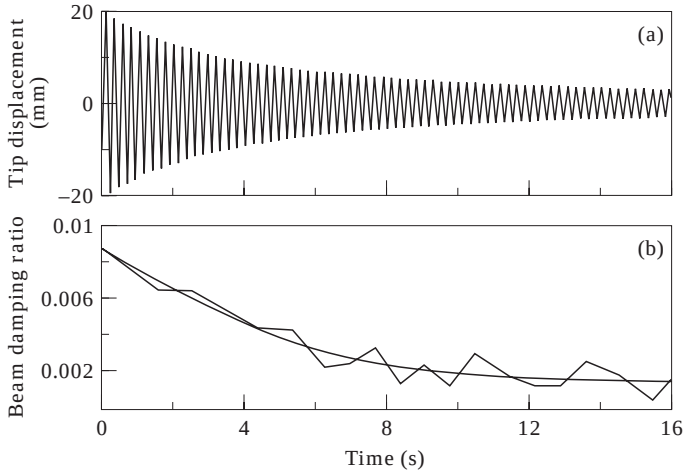

Figure 8. (a) Free vibration of the beam, (b) beam damping.

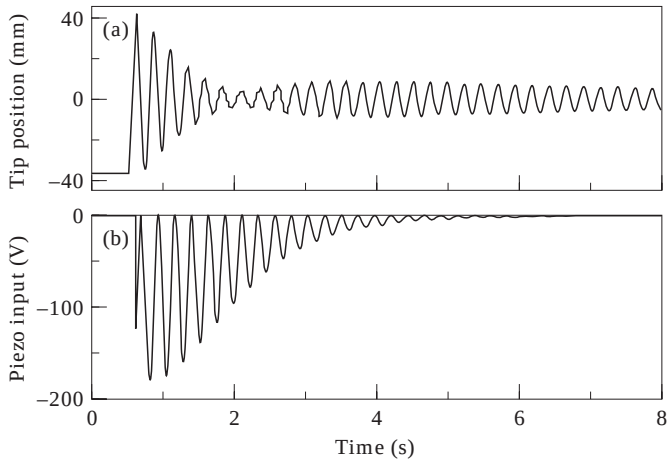

Figure 9. (a) Neck in the beam response, (b) input voltage to the piezo-ceramics.

in Figure 11. The results indicate that the proposed controller is robust enough to be used in practical applications.

For comparison, the beam response with a velocity feedback controller was examined. It should be noted that the beam input u_p (piezo-ceramics input) was not filtered when one applied the proposed MCC. However, when one attempted to implement the velocity feedback controller to the beam the input signal had to be filtered. The controller was unstable unless the beam input was filtered with a low pass filter with a cut off frequency lower than 24 Hz.

The velocity gain was selected so that for beam oscillations with amplitude ± 40 mm, the input to the piezo-ceramics becomes ± 180 V. In Figure 12(a) the dashed line shows the beam response with velocity feedback while the solid line indicates the beam response with the proposed MCC. The piezo-ceramics input is shown in Figure 12(b). The dashed and solid lines present the piezo-ceramic input using velocity feedback and MCC, respectively.

Although the beam response with the velocity feedback controller is damped slightly faster in the first five cycles, the beam amplitude is the same for both controllers afterward.

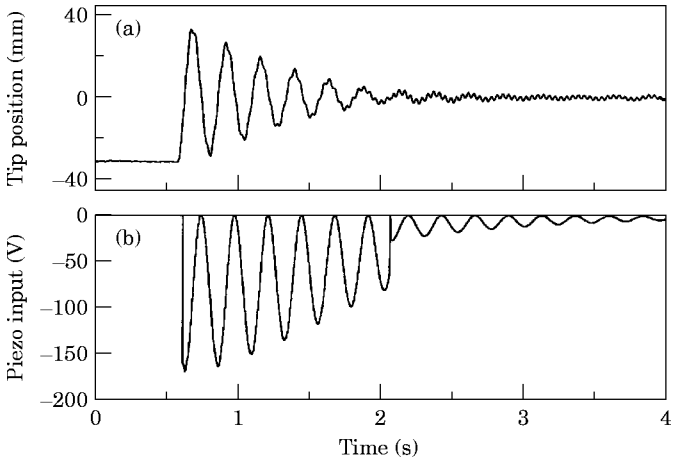

Figure 10. (a) Beam response using UIA, (b) input voltage to the piezo-ceramics.

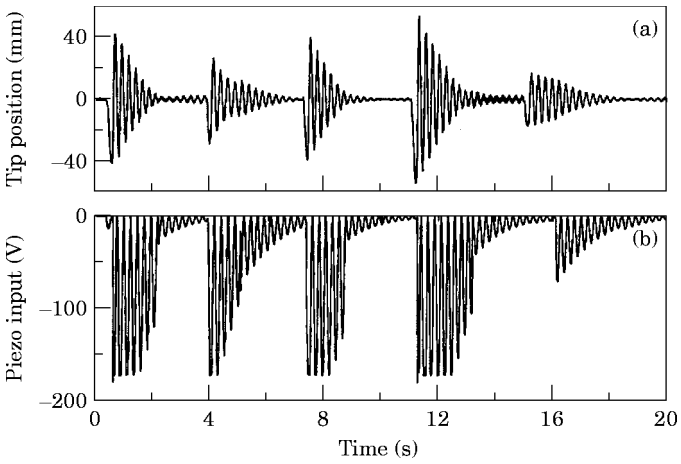

Figure 11. (a) Beam response using UIA with disturbance, (b) input voltage to the piezo-ceramics.

It is also well worth noticing that while the input of the MCC varies between -180 and 0 V, the input of the velocity feedback changes between -180 and 180 V; the overall performance of the controllers is the same.

As another comparison, a uni-directional velocity feedback controller is applied to the beam. In this controller the piezo-ceramics input is set to zero whenever $\dot{x}_p < 0$. In Figures 13(a) and (b) the dashed and solid lines indicate the beam response and piezo-ceramics input using the uni-directional velocity feedback and MCC, respectively. From the plots it is obvious that although the maximum actuator effort for both controllers is the same, the beam response is suppressed more rapidly using the proposed MCC. This is the most significant advantage of the MCC over conventional control methods for actuators which are not able to produce a symmetric force. Examples of these actuators are cable-driven and shape memory alloys actuators. Since the method is able to produce a uni-directional input, it can be utilized more effectively with this type of actuators.

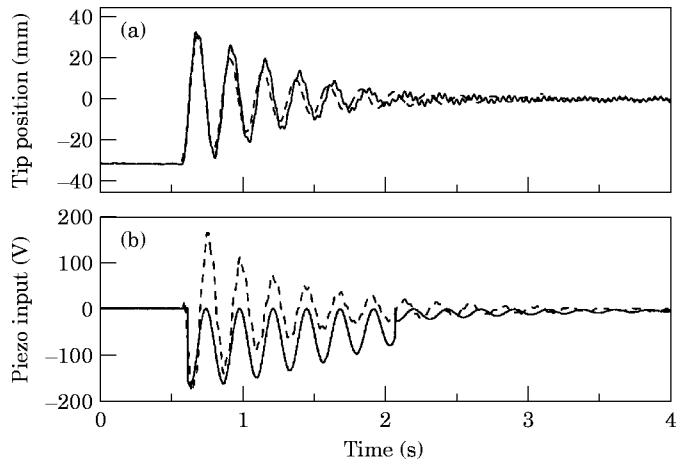

Figure 12. (a) Comparison of the beam response using MCC (——) and velocity feedback (- - - -). (b) Input voltage to the piezo-ceramics using MCC (——) and velocity feedback (- - - -).

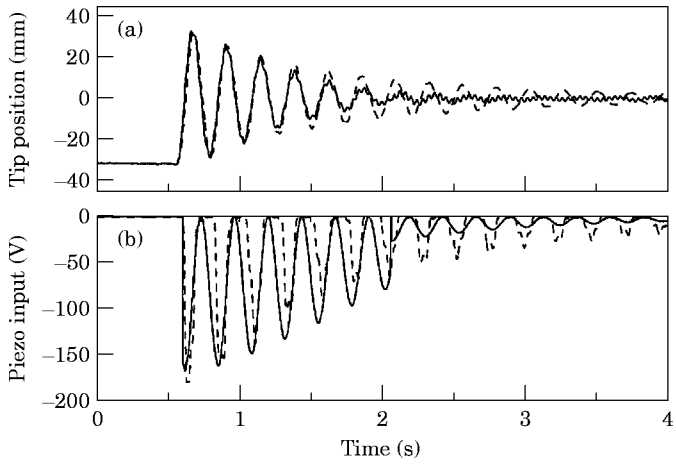

Figure 13. (a) Comparison of the beam response using MCC (——) and uni-directional feedback (- - - -). (b) Input voltage to the piezo-ceramics using MCC (——) and uni-directional feedback (- - - -).

7. CONCLUSION

In this two-part paper, a new method in non-linear controller design has been studied using the notion of non-linear modal coupling. All theoretical aspects of the proposed technique have been elaborated and shows that for a wide class of non-linear systems with oscillatory linear part, the method can be applied. The stability of the closed loop system has also been addressed and a simple relation to test the stability of the system derived.

The **U**pgrading **I**nput **A**lgorithm (UIA) has been introduced as a means to implement the controller. The algorithm takes advantage of the neck which is developed in the plant response. The method was applied to an experimental flexible beam. The results show that the proposed MCC is more robust to noise. Furthermore, the proposed controller is able to produce a uni-directional input which has the same performance, using a velocity feedback control, with twice the peak to peak actuator effort. This is particularly useful for the cases where the actuators are uni-directional.

REFERENCES

1. A. Khajepour, M. F. Golnaraghi and K. A. Morris 1997 *The Journal of Sound and Vibration* **205,** 657–670. Model coupling controller design using a normal form method, part I: dynamics.
2. M. F. Golnaraghi 1991 *Dynamics and Control*, **1**, 405–428. Regulation of flexible structure via nonlinear coupling.
3. M. F. Golnaraghi, K. Tuer and D. Wang 1994 *Dynamics and Control* **4**, 73–96. Regulation of lumped parameter cantilever beam via internal resonance using coupling enhancement.
4. J. Guckenheimer and P. Holmes 1983 *Nonlinear Oscillations, Dynamical Systems and Bifurcations of Vector Fields*. New York: Springer Verlag.
5. A. Khajepour, M. F. Golnaraghi and K. A. Morris 1994 *Proceedings of the ASME International Mechanical Engineering Congress and Exposition*, AMD **192**/DE **78**, 143–150. Internal resonance controller design using normal forms.
6. A. Khajepour, M. F. Golnaraghi and K. A. Morris 1995 *Proceedings of the ASME Design Engineering Technical Conferences*, DE 84-1, **3**, 477–485. Vibration suppression of a flexible beam using center manifold theory.
7. V. I. Arnold 1987 *Geometrical Methods in the Theory of Differential Equations*. New York: Springer Verlag.
8. A. Khajepour, M. F. Golnaraghi and K. A. Morris 1997 *The ASME Journal*

of Vibration and Acoustics **119,** 158–166. Application of center manifold theory to regulation of a flexible beam.
9. S. S. Oueini and M. F. Golnaraghi 1996 *The Journal of Sound and Vibration* **191,** 377–396. Experimental implementation of the internal resonance control strategy.
10. K. Tuer, M. F. Golnaraghi and D. Wang 1995 *IEEE Transaction on Automatic Control* **40**, 522–530. Toward a generalized regulation scheme for oscillatory systems via coupling effects.
11. S. Wiggins 1990 *Introduction to Applied Nonlinear Dynamical Systems and Chaos*. New York: Springer Verlag.
12. M. Vidyasagar 1993 *Nonlinear System Analysis*. NJ: Prentice Hall.
13. J. J. E. Slotine and W. Li 1991 *Applied Nonlinear Control*. NJ: Prentice Hall.
14. A. H. Nayfeh and D. T. Mook 1978 *Nonlinear Oscillations*. New York: Wiley-Interscience.

APPENDIX A: GENERAL FORMS OF TERMS IN EQUATION (40)

The general form of a_0, a_1, b_0, b_1 and d in equation (40) are

$$a_0 = -9(w_c \sin(2\phi_c)q_4 + \beta_c \cos(2\phi_c)q_3)p_2^2 + 18w_c(\sin(2\phi_c)q_3 - \beta_3 w_c \cos(2\phi_c)q_4)p_2p_3 + 9w_c^2(\beta_c \cos(2\phi_c)q_3 + \sin(2\phi_c)w_c q_4)p_3^2, \tag{A.1}$$

$$\begin{aligned} a_1 = {} & (18p_3^2(\sin(4\phi_c) - 3\sin(2\phi_c))w_c^2 + 9\beta_c p_2p_3(7\cos(2\phi_c) - 4\cos(4\phi_c))w_c \\ & + 9p_2^2(\sin(2\phi_c) - 2\sin(4\phi_c))q_3 + 3w_c(6\beta_c p_3^2(\cos(4\phi_c) - 1)w_c^2 \\ & + 3p_2p_3(4\sin(4\phi_c) + 3\sin(2\phi_c))w_c - \beta_c p_2^2(6\cos(4\phi_c) + 9\cos(2\phi_c) + 6))q_4 \\ & + 6w_c(\beta_c p_3^2(3\cos(2\phi_c) - 2\cos(4\phi_c))w_c^2 + p_2p_3(3\sin(2\phi_c) \\ & - 4\sin(4\phi_c))w_c + 2\beta_c p_2^2\cos(4\phi_c))r_2 + 24w_c^2(\sin(4\phi_c)(p_3^2w_c^2 - p_2^2) \\ & - 2\beta_c p_2p_3w_c\cos(4\phi_c))r_3 + 3(p_3^2(3\sin(2\phi_c) - \sin(4\phi_c))w_c^2 \\ & + p_2p_3\beta_c(2\cos(4\phi_c) - 3\cos(2\phi_c))w_c + p_2^2\sin(4\phi_c))r_2' \\ & + 6w_c(\beta_c p_3^2(3 - \cos(4\phi_c))w_c^2 - 2p_2p_3\sin(4\phi_c)w_c + \beta_c p_2^2(3 + \cos(4\phi_c))r_3', \end{aligned} \tag{A.2}$$

$$b_0 = 9(\beta_c \sin(2\phi_c)q_3 - w_c \cos(2\phi_c)q_4)p_2^2 + 18w_c(\cos(2\phi_c)q_3 + \beta_c w_c \sin(2\phi_c)q_4)p_2p_3 + 9w_c^2(w_c \cos(2\phi_c)q_4 - \beta_c \sin(2\phi_c)q_3)p_3^2, \tag{A.3}$$

$$\begin{aligned} b_1 = {} & 9(2p_3^2(\cos(4\phi_c) - 2\cos(2\phi_c) - 1)w_c^2 + \beta_c p_2p_3(4\sin(4\phi_c) - 7\sin(2\phi_c))w_c \\ & + p_2^2(3\cos(2\phi_c) - 2\cos(4\phi_c) - 2))q_3 + 3w_c(-6\beta_c p_3^2(\sin(4\phi_c) + \sin(2\phi_c))w_c^2 \\ & + p_2p_3(9\cos(2\phi_c) + 12\cos(4\phi_c))w_c + 3\beta_c p_2^2(2\sin(4\phi_c) + \sin(2\phi_c)))q_4 \\ & + 6w_c(\beta_c p_3^2(\sin(4\phi_c) - 3\sin(2\phi_c))w_c^2 + p_2p_3(3\cos(2\phi_c) - 2\cos(4\phi_c))w_c \\ & - \beta_c p_2^2\sin(4\phi_c))r_2 + 6w_c^2(2p_3^2(\cos(4\phi_c) - 3)w_c^2 + 4\beta_c p_2p_3w_c\sin(4\phi_c) \\ & - 2p_2^2(\cos(4\phi_c) + 3))r_3 + 3(p_3^2(3\cos(2\phi_c) - 2\cos(4\phi_c))w_c^2 + p_2p_3\beta_c(3\sin(2\phi_c) \\ & - 4\sin(4\phi_c))w_c + 2p_2^2\cos(4\phi_c))r_2' + 6w_c(2\beta_c\sin(4\phi_c)p_3^2w_c^2 - 4p_2p_3\cos(4\phi_c)w_c \\ & - 2\beta_c p_2^2\sin(4\phi_c))r_3', \end{aligned} \tag{A.4}$$

$$d = 64\beta_c\zeta_c^3(3\zeta_c^2 + 1)(5\zeta_c^2 - 9)(3\zeta_c^2 - 4)^2w_c^3. \tag{A.5}$$